ROME1-1389-2004

SUSY Resonances from UHE neutralinos in Neutrino Telescopes and in the Sky

Anindya Datta, Daniele Fargion, and Barbara Mele [1]

INFN, Sezione di Roma, and
Dip. di Fisica, Università La Sapienza, P. le A. Moro 2, I-00185, Rome, Italy.

Abstract

In the *Top-down* scenarios, the decay of super-heavy particles ($m \sim 10^{12-16}$GeV), situated in dark-matter halos not very far from our Galaxy, can explain the ultra-high-energy (UHE) cosmic-ray spectrum beyond the Griesen-Zatasepin-Kuzmin cut-off. In case the dynamics of this decay is governed by the minimal supersymmetric standard model, a major component of the UHE cosmic-ray flux at PeV-EeV energies could be given by the lightest *neutralino* χ_1^0, that is the lightest stable supersymmetric particle. Then, the signal of UHE χ_1^0's on earth might emerge over the interactions of a comparable neutrino component. We compute the event rates for the resonant production of *right selectrons* ($\tilde{e}_R$) and *right squarks* ($\tilde{q}_R$) in mSUGRA, when UHE neutralinos of energy $E_\chi \gtrsim 10^5$ GeV scatter off electrons and quarks in an earth-based detector like IceCube. When the resonant channel dominates in the total $\chi_1^0 e, \chi_1^0 q$ scattering cross section, the only model parameters affecting the corresponding visible signal rates turn out to be the physical masses of the resonant right-scalar and of the lightest neutralino. We compare the expected number of supersymmetric events with the rates corresponding to the expected Glashow W resonance and to the continuum UHE νN scattering for realistic power-law spectra. We find that the event rate in the leptonic selectron channel is particularly promising, and can reach a few tens for a one-year exposure in IceCube. Finally, we note that UHE neutralinos at much higher energies (up to hundreds ZeV) may produce *sneutrino* ($\tilde{\nu}$) resonances by scattering off relic neutrinos in the Local Group hot dark halo. The consequent $\tilde{\nu}$ *burst* into hadronic final states could mimic *Z-burst* events, although with quite smaller conversion efficiency.

1 Introduction

The presence of a ultra-high-energy (UHE) component in the cosmic-ray spectra beyond the Griesen-Zatasepin-Kuzmin cutoff (GZK) [1], as revealed initially by the experiment Fly's Eye [2], subsequently by AGASA [3], and marginally by Hires [4], is presently an open problem in high-energy astrophysics. The highest-energy particles in the cosmic-ray spectrum are apparently protons rather than photons, because of their characteristic hadronic-shower fluorescence light shapes. Beyond the GZK energies, protons, slowed down by the cosmic Black Body Radiation, have energy-loss length well below 50 Mpc. This implies that possible sources of these extremely-high-energy particles should be within our Galaxy, or inside our Local Group

[1] E-mail: Anindya.Datta@roma1.infn.it, Daniele.Fargion@roma1.infn.it, Barbara.Mele@roma1.infn.it

of Galaxies or nearby Clusters. However, there are no such powerful sources in Milky Way or nearby Virgo Group, that are correlated with the arrival map of the UHE cosmic rays (UHECR). There is a timid, and yet unconfirmed, clustering of AGASA data along the Super-Galactic Plane, not sufficient to probe the UHECR confinement in observable GZK volumes. On the contrary, UHECR events exhibit isotropy, a signature reminiscent of most distant cosmic edges. It is not clear whether the UHECR spectrum is really showing a GZK cut-off [3, 4]. In order to make our UHECR understanding even more confused, there are now first evidences of clustered UHECR events by AGASA correlated with known BL Lacs sources [5]. This UHECR-BL Lacs connection calls for the UHE Blazing Jet of active galactic nuclei (AGN) as a source of particle acceleration. Those Bl Lacs sources are mostly at distances above GZK lengths.

Although the GZK puzzle is still experimentally not completely settled, in the past and also recently, there have been quite a few suggestions about possible sources and mechanisms for accelerating particles to such extreme energies [6, 7].
A class of proposals, generically called *Top-down* scenarios, tries to explain the high-energy part of the spectrum through the decay of super-massive particles ($m \sim 10^{12-16}$GeV) [8, 9, 10, 11, 12], or by their eventual binary collapse and annihilation in place of time-tuned decays [13]. These particles are generally predicted in Grand Unified Theories (GUT). Their decay lifetime should be comparable with the present age of the Universe, so that their decay products would give rise today to the highest energy part of the cosmic-ray spectrum. Also topological defect decays can give rise to the UHECR primaries [6]. In any case, the decay dynamics of the super-heavy particles is controlled by the model assumed for particle interactions. In the standard model (SM), the decay after fragmentation finally results into photons, neutrinos and hadrons. In supersymmetry (SUSY), UHE secondary stable neutralinos (χ_1^0) may be born, too [9, 10, 11, 12].

The minimal supersymmetric standard model (MSSM) is a well motivated extension of the standard model of elementary particles [14]. SUSY stabilizes the Higgs-boson mass under radiative corrections by introducing an entire spectrum of supersymmetric partners for the SM particles. The MSSM predicts a stable weakly-interacting heavy neutral particle, called neutralino (χ_1^0), which can be also a good candidate for cold dark matter[2]. If the masses of supersymmetric particles are at the TeV scale (as needed to stabilize the Higgs-boson mass), we expect to discover them in a few years at the CERN LHC [15]. In the case SUSY is the correct theory of particle interactions, it will govern also the decays of super-heavy particles. In [10, 11, 12], the super-heavy particle decays in the MSSM extension of the SM have been investigated in detail. These decays would involve the entire spectrum of SUSY partners. At the end of the decay chain, one would be left with a spectrum (calculable in the MSSM) of all the stable particles, that is SM particles plus stable neutralinos. Hence, a crucial prediction of these models is the presence of neutralinos in the UHECR spectrum produced by super-heavy objects.

Another possible explanation for the GZK paradox considers relic light neutrinos as a calorimeter in resonance with incoming UHE (ZeVs) neutrinos. The latter may come freely from distances above GZK from far BL Lacs (hence explaining the UHECR-BL Lacs correlations) or gamma ray bursts (GRB). They may also arise from topological defects spread all over dark halos (Galactic or extra-galactic). This model, the so-called *Z-burst* model [16] will be discussed in the following in view of a new and analogous *sneutrino*-burst model.

[2]In general, in the MSSM, there are 4 neutralinos. Here, we are talking about the lightest one χ_1^0.

According to the discussion above, we shall assume in this study a rather hard neutralino spectrum (i.e. $\sim E_\chi^{-1.5}$) that should be typical for the GUT-relics fragmentation. In order to estimate the effects of model dependence in the spectral index, we will also compare our results with the ones corresponding to a softer *Fermi-like* flat spectrum, going as $\sim E_\chi^{-2}$. We shall not consider a much harder *Z-burst*−like spectrum ($\sim E_\chi^{-1}$) that is usually used in different context, although such a spectrum could be of relevance for a *sneutrino*-burst model.

One of the major goals for the upcoming UHECR experiments (like Amanda, IceCube, Antares, Nestor) is to verify these predictions. In [17], the possible signatures of up-going UHE neutralinos in the future satellite-based detector EUSO [18] have been investigated. The resonant production of quite heavy squarks ($m \sim 0.8 - 1.2$ TeV) in the χ_1^0 scattering off nucleons in the earth's atmosphere, after crossing all the earth volume, has been considered. Heavy squarks are selected so that the neutralino interaction cross sections are moderate, and the neutralino flux is not completely stopped by the earth screen (while the corresponding neutrino background does not survive the passage through the earth). An analogous process leading to a smaller neutrino earth opacity has been also considered earlier, while discussing the up-going τ neutrinos [19]. Note that, in EUSO, the UHE neutralino interaction in the atmosphere is polluted by more abundant up-going-horizontal τ air-showers induced by UHE ν_τ earth skimming in the terrestrial crust [20].

In the present article, we will focus on the interaction of the highest energy neutralinos with both electrons and nucleons in a earth-based detector like IceCube [21]. In particular, we will study the possibility to detect the resonant production of the SUSY partners of electrons and quarks, when their masses are larger than the present experimental limits derived from direct searches at high-energy colliders ($m_{\tilde{e}} \gtrsim 100$ GeV for selectrons [22], $m_{\tilde{q}} \gtrsim 300$ GeV for squarks[3] [23]). We will also take into account the constraints on the supersymmetry parameter space coming from bounds on the relic density of the lightest neutralino, in case the latter is responsible for most of the cold dark matter in the universe.

Neutralinos with appropriate energy can produce a right/left selectron ($\tilde{e}_R/\tilde{e}_L$) resonance in the detector via the scattering off the detector electrons

$$\chi_1^0 + e^- \to \tilde{e}_{R,L} \to X$$

(see Fig. 1). Here, X stands for some visible final state arising from the $\tilde{e}_{R,L}$ decay, that will be eventually revealed by the detector. As far as the scalar mass is not too heavy and χ_1^0 has a relevant gaugino component, for resonant χ_1^0 energies this channel gives the dominant contribution to the scattering cross section, and one can neglect t-channel effects.
The kinematics and signature is somehow similar to the W^- resonant production in UHE antineutrino-electron scattering [24]

$$\bar{\nu}_e + e^- \to W^- \to X \ ,$$

that is expected to occur at the *Glashow* resonant energy $E_\nu = M_W^2/(2m_e) \simeq 6.3$ PeV. Since we can predict the exact characteristics of this channel (like its hadronic and electromagnetic showering and its final visible energies), the corresponding events could be used to calibrate the SUSY resonance observation.

Right/left-squark ($\tilde{q}_R/\tilde{q}_L$) resonances can be produced through the neutralino scattering off the quarks in the detector nucleons

$$\chi_1^0 + q \to \tilde{q}_{R,L} \to X \ .$$

[3]Even lighter squarks are allowed for $m_{\tilde{g}} \gg m_{\tilde{q}}$.

Although, at the partonic level, this process has the same resonant structure as the selectron channel, due to the quark momentum spread inside the nucleon, the cross-section resonance peak is smeared, and the χ_1^0 incident-energy resonant characteristics are lost.

The background coming from the UHE ν interaction with nucleons ($\nu + q \to X$) by t-channel processes could create a major continuous background overlapping or overshadowing the squark signal. In the following, after computing the relevant χ_1^0 event rates, we will address the issue of disentangling the SUSY signal from the SM resonant and continuous background given by the competitive UHE neutrinos.

Higher-energy neutralinos [with $E_\chi \sim m_{\tilde{\nu}}^2/(2m_\nu)$] could interact with light relic neutrinos in the Local Group or Super-Galactic Plane, and produce sneutrino $\tilde{\nu}$ resonances in the process [25]

$$\chi_1^0 + \nu \to \tilde{\nu} \to X \ .$$

The following sneutrino decay into final states containing hadrons can in principle mimic a *Z-burst* event [16]. In this paper, we will also go through a *$\tilde{\nu}$-burst* scenario.

While calculating the neutralino scattering cross-sections, we will stick to a particular model of SUSY breaking, namely the minimal supergravity mediated model (mSUGRA) [26]. The mSUGRA and its variants are theoretically well motivated. The parameter space of mSUGRA is characterized by five quantities: m_0 and $m_{1/2}$, the universal scalar and gaugino masses, respectively; A_0, the universal trilinear scalar coupling (all taken at the scale of grand unification); $\tan\beta$, the ratio of the vacuum expectation values of the two Higgs doublets; the sign of μ, the Higgs mixing parameter ($\mathcal{W} \ni \mu H_1 H_2$, where H_1, H_2 are the two higgs superfields in the superpotential $\mathcal{W}$). While the sign of μ is arbitrary, its magnitude is determined by requiring the radiative electroweak symmetry breaking.

In most of the mSUGRA parameter space, the lightest neutralino is almost a pure bino $\tilde{B}$, the superpartner of the $U(1)$ gauge field [4]. This is particularly important for χ_1^0 being a good candidate for cold dark matter [27]. Then, the *right* slepton and *right* squark are maximally coupled to the lightest neutralino, and resonant $\chi_1^0 f \to \tilde{f}_R$ cross sections are in general enhanced with respect to $\chi_1^0 f \to \tilde{f}_L$ cross sections (where $f = e, q$).

We will then restrict our study to the right-scalar resonant production and decay into the same initial particles $\chi_1^0 f$. The corresponding production rates will turn out to be quite straightforward to compute, the only critical parameters being the physical masses of the particle involved in the process (that is the resonance and neutralino masses, $m_{\tilde{f}_R}$ and m_χ). In any case, one should keep in mind that the model predicts further new channels associated to the left scalar resonances (sort of *twin shadows* of the right scalars) whose rate is in general suppressed with respect to the right scalar by both the lower (and in general more model-dependent) relevant decay branching fractions (see Section 3), and the heavier resonance masses (since in general $m_{\tilde{f}_L} \gtrsim m_{\tilde{f}_R}$).

The neutralino energies that are relevant for the resonant reactions $\chi_1^0 q \to \tilde{q}$, $\chi_1^0 e \to \tilde{e}$, $\chi_1^0 \nu \to \tilde{\nu}$ are strictly determined by the resonance and target masses [$E_\chi \sim m_{\tilde{f}}^2/(2m_{target})$], that is

$$E_\chi \quad \gtrsim \quad \frac{m_{\tilde{q}}^2}{2m_p} \sim 10^5 \ \text{GeV}, \tag{1}$$

[4] In general, a neutralino is a linear combination of the two Higgs superpartners $\tilde{H}_1$, $\tilde{H}_2$ (higgsinos), a $\tilde{W}_3$ (wino) and a $\tilde{B}$ (bino).

$$E_\chi \sim \frac{m_{\tilde{e}}^2}{2m_e} \simeq 10^7 \div 10^9 \text{ GeV}, \quad (2)$$

$$E_\chi \sim \frac{m_{\tilde{\nu}}^2}{2m_\nu} \simeq 10^{14} \text{ GeV}, \quad (3)$$

respectively (m_p, m_e, m_ν being the proton, electron, relic-neutrino masses), where we assumed $m_{\tilde{q}} > 300$ GeV, $m_{\tilde{e}} \simeq 100 - 1000$ GeV, $m_{\tilde{\nu}} \simeq 200$ GeV, and $m_\nu \simeq 0.1$ eV.

The plan of this paper is the following. In Section 2, we discuss our assumptions on the UHE-neutralino spectrum. In Section 3, we present the cross-sections for the UHE-neutralino interaction with electrons and quarks leading to selectron and squark resonances. In Section 4, we present the event rates for the selectron and squark resonant production by UHE χ_1^0 for a 1-km^3 ice detector, in benchmark mSUGRA scenarios that takes into account cosmological bounds on the neutralino relic density. They will then be compared with the number of events expected to arise from the *Glashow* resonance $\bar{\nu}_e e \to W^-$, and from the $\nu(\bar{\nu})-$nucleon interaction via charged- and neutral-current processes, assuming comparable UHE-neutrino and neutralino spectra. In Section 5, we address the issue of disentangling the SUSY events in the detector by looking at their peculiar energy spectrum and fluence for visible decay products. In Section 6, we will discuss a possible $\tilde{\nu}$-*burst* scenario, corresponding to the resonant interaction of UHE χ_1^0's with light relic neutrinos in the Local Group or SuperCluster hot dark halos. Finally, in Section 7, we present our conclusions.

2 The UHE-neutralino spectrum

In this section, we will discuss our assumptions regarding the neutralino flux in the UHECR. In our study, we are mainly concerned with models of SUSY-driven decays of super-heavy particles. Different studies in the literature show that the final neutralino spectrum is quite dependent on the specific fragmentation model [10, 11, 12]. Here, we will not adopt any specific fragmentation model, but we will follow a more phenomenological approach. We will try to keep our study as model independent as possible by assuming for the neutralino flux a -1.5 spectral index, that should be typical of the fragmentation of heavy objects. The results of a switch to a -2 index are also analyzed, in order to estimate the effects of the expected uncertainty in the predicted spectral index. Regarding the flux normalization, we will be only guided by present and projected experimental limits on UHE neutrino fluxes.

Neutrinos and neutralinos of comparable energies , while interacting with matter, will produce somewhat similar signals in an earth-bound detector. In general, neutralino-interaction rates are expected to be smaller than the neutrino ones. This implies *less stringent* experimental bounds on neutralino fluxes with respect to neutrino fluxes. Although there would be some room for a more abundant incoming UHE-neutralino flux, we will assume, for the sake of simplicity and with a conservative attitude, comparable UHE neutralino and neutrino fluxes, that is $\phi_\chi \sim \phi_\nu$. We will then directly turn present neutrino flux bounds into neutralino flux limits. Concerning the range of energies we are interested in for selectron and squark resonances (i.e., $E_\chi \sim (1 - 10^3)$ PeV), AMANDA gives the most stringent experimental limit on neutrino fluxes for energies lower than 5 PeV [28]. In the higher range, upper bounds on the UHE neutrino flux comes also from AGASA [3], Flys Eye [2], and RICE [29].

In particular, from the study of a possible excess in cascade events and assuming relative flavor abundances $\nu_e : \nu_\mu : \nu_\tau = 1 : 1 : 1$, AMANDA sets a limit on the total neutrino

flux of $E_\nu^2 \frac{dN}{dE_\nu} \simeq 8.6 \times 10^{-7}$ GeV cm^{-2} s^{-1} sr^{-1}, for 50 TeV$< E_\nu <$ 5 PeV, and $\simeq 1.5 \times 10^{-6}$ GeV cm^{-2} s^{-1} sr^{-1}, for 1 PeV$< E_\nu <$ 3 EeV [28].

For comparable interaction strength of neutrinos and neutralinos with matter, neutralino fluxes as high as the above limits are allowed, while weaker neutralino interactions allow even larger spectra.

In our study, we will assume that the neutralino flux is comparable with the flux of just one neutrino species, *i.e.* $\phi_\chi \simeq \phi_{\nu_i+\bar{\nu}_i}$ $(i = e, \mu, \tau)$. This hypothesis is somehow conservative, since, in models of super-heavy particle decays, one can have scenarios where the neutralino fluxes are even larger than the sum of all the neutrino components in the upper energy range [12].

Regarding the neutralino flux shape (or spectral index), we will model it according to the typical behavior of present predictions for neutralino fluxes arising from the fragmentation of super-heavy objects [10, 11, 12].

Models of UHECR fluxes arising from super-heavy X particle decays have been mainly motivated by the GZK puzzle. In order to have an appreciable X decay rate today, one has to tune the X lifetime to be longer (but not too much longer) than the age of the universe, or else *store* short-lived X-particles in topological vestiges of early universe phase transitions. Then, the estimate of the X lifetime and volume density is very model dependent. Furthermore, the internal mechanisms of the decay and the detailed dynamics of the first secondaries do depend on the exact nature of the particles.

Consequently, *no firm prediction* on the expected flux of neutralinos can be made. However, if there are no new mass scales between $M_{\rm SUSY} \sim 1$ TeV and M_X, the squark and sleptons behave like their corresponding supersymmetric partners. Then, one can infer the gross features of the X-particle cascade from the *known* evolution of quarks and leptons.

The upper edge of the neutralino distribution would be then connected to the super-heavy particle mass M_X. In the analysis of a super-massive object decay in [12], the neutralino spectrum goes down with the energy as $E^{-1.3}$, and extends up to about $E \sim M_X/2$.

At large energy fractions $x \equiv 2E/M_X$, the χ_1^0 flux tends to be comparable or even larger that the ν flux. In particular, for $x > (0.1 - 0.5)$ (depending on the particular fragmentation treatment [10, 11, 12]) neutralino and neutrino fluxes are in general comparable, while at $x < 0.1$ neutralinos are depleted with respect to neutrinos. Also, the total energy carried away by the neutralinos can be comparable with that of the neutrinos. In fact, when the *initial decay* of the X particle is into SUSY particles, the total energy of the decay carried by the neutralinos can be even larger than the neutrino energy (see, e.g., Tables 2.1, 2.2 and 2.3 in the last reference in [12]).

Consequently, the neutralino flux in the energy range relevant for resonant production of selectron and squarks [i.e. $E_\chi \sim 10^{6-9}$ GeV, see eq. (1),(2)], could be quite depleted when supposing $M_X \sim 10^{12-16}$ GeV in order to explain the GZK puzzle, implying neutralino energy fractions $x < 0.001$.

For instance, assuming $M_X \simeq 2 \times 10^{12}$ GeV to fit the GZK cosmic rays data (see Fig. 1 in [17]), and using the fragmentation model in [12], one gets neutralino fluxes of the order of $E_\chi^2 \frac{dN}{dE_\chi} = 10^{-8}$ GeV cm^{-2} s^{-1} sr^{-1} at $E_\chi \simeq 10^2$ PeV (see Fig. 2 in [17]). This flux would be more than one order of magnitude smaller than the value that can be extrapolated from present experimental upper bounds on neutrino fluxes at lower energies, assuming, as in [17], a $E^{-1.3}$ spectral behavior.

On the other hand, a lighter X-particle mass in the range 10^{8-9} GeV (as considered for

instance in [30]) would provide a more appropriate setting for resonant selectron and squark production, enhancing the neutralino flux up to a level close to neutrino fluxes in the 10^{7-9} GeV energy range. A M_X value in the 10^{8-9} GeV ballpark would not be in conflict with any theoretical or experimental consideration, although it would be less interesting in view of a possible explanation of the GZK puzzle.

Anyhow, we stress that at the present stage one could also think of models the can reconcile the 'low' energy range needed for resonant selectron and squark scattering with the 'large' M_X value fitting the GZK energy range. For instance, assuming for the heavy X object a lifetime shorter than the one of the Universe, one would presently expect a tail of redshifted secondaries. If the X decay occurs smoothly at redshift $10^3 \gtrsim z \gtrsim 1$, then the peak X decays at largest redshift ($z \sim 10^3$) even in the case $M_X \sim 10^{12}$ GeV would eject its neutralino component at a lower energy of the order $E_\chi \simeq M_X/[2(1+z)] \simeq 10^9$ GeV today.

All the previous considerations converge in our choice of a "reference" neutralino flux given by a fragmentation-like power law with spectral index -1.5, and normalization well compatible with the AMANDA bounds :

$$E_\chi^2 \frac{dN}{dE_\chi} = 10^{-7} \text{ GeV cm}^{-2} \text{ s}^{-1} \text{ sr}^{-1} \left[\frac{E_\chi}{10^7\ GeV}\right]^{0.5} . \tag{4}$$

Although one could easily build up models matching the above "reference" normalization, in the following analysis it will be straightforward to rescale our results on expected event numbers according to a possible more conservative (smaller) normalization factor in eq. (4).

In order to assess the effect of the uncertainty in the spectral index arising from differences in modeling the super-heavy object fragmentation, we also considered, for comparison, a Fermi-like neutralino flux with spectral index -2 :

$$E_\chi^2 \frac{dN}{dE_\chi} = 10^{-7} \text{ GeV cm}^{-2} \text{ s}^{-1} \text{ sr}^{-1}, \tag{5}$$

whose normalization is also compatible with experimental neutrino limits. We than compared event numbers relative to eqs. (4) and (5).

Summarizing this section, the details of UHE neutrinos and neutralinos fluxes are quite model dependent, and we are in a very preliminary understanding of their possible spectra. Hence, we decided to use two phenomenological assumptions for the UHE neutralino spectrum differing by the spectral index, and reflecting possible differences in modeling the fragmentation of a super-heavy object. In both cases, the flux normalization has been fixed on the basis of present UHE neutrino experimental bounds. This hypothesis could be quite conservative, since the lower neutralino-nucleon cross section ($\sigma_{\chi N} \lesssim \frac{1}{10}\sigma_{\nu N}$, see Section 4) would make any possible astrophysical source of UHE neutrinos and neutralinos more transparent to (and hence more efficient in producing) the χ_1^0 component.

Assuming a different normalization in eqs. (4) and (5) will simply imply the rescaling of the event numbers obtained in our final analysis.

3 Resonant cross sections for UHE neutralino interactions with matter

UHE neutralinos with proper energy will interact with the electrons and quarks inside the detector, and produce selectron or squark resonances via $\chi_1^0 + (e^-, q) \to (\tilde{e}, \tilde{q}) \to X$ (see the

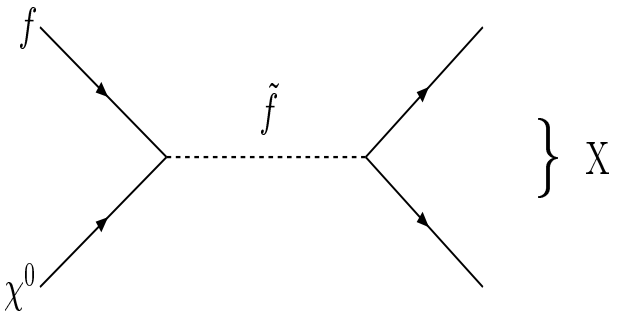

Figure 1: Feynman diagram of the process $\chi_1^0 + f \to \tilde{f} \to X$, where f can be an electron, a quark or a neutrino.

Feynman diagram in Fig. 1, where f is either a lepton or a quark). The symbol X stands for a given *visible* final state arising from the $\tilde{f}$ decay.

Near the resonance, the cross-section σ of the process can be written in terms of the particle masses and the $f\chi_1^0$ center-of-mass (c.m.) energy s in the Breit-Wigner approximation

$$\sigma(s) = 2\pi \, \frac{1}{|\mathbf{k}|^2} \, \frac{s \, \Gamma_{\tilde{f}}^2}{(s - m_{\tilde{f}}^2) + m_{\tilde{f}}^2 \Gamma_{\tilde{f}}^2} \, B(\tilde{f} \to f \, \chi_1^0) \, B(\tilde{f} \to X) \, . \tag{6}$$

In the equation above, $m_{\tilde{f}}$ is the slepton/squark mass, $\Gamma_{\tilde{f}}$ is its total decay width, and $B(\tilde{f} \to f \, \chi_1^0)$, $B(\tilde{f} \to X)$ are their decay branching fractions $[B(\tilde{f} \to \ldots) \equiv \Gamma(\tilde{f} \to \ldots)/\Gamma_{\tilde{f}}]$ into the final states $f \, \chi_1^0$ and X, respectively. The modulus of the c.m. 3-momentum of the initial particles $\mathbf{k}$ can be expressed as

$$|\mathbf{k}| = \frac{m_{\tilde{f}}^2 - m_\chi^2}{2m_{\tilde{f}}} \tag{7}$$

where m_χ is the neutralino mass. Then, the c.m. energy s is related to the incident neutralino energy E_χ in the laboratory by

$$s = m_\chi^2 + 2m_f E_\chi, \tag{8}$$

where m_f is the target mass. At the resonance ($s \sim m_{\tilde{f}}^2$), the neutralino energy is then

$$E_\chi^{peak} \simeq \frac{m_{\tilde{f}}^2 - m_\chi^2}{2m_f}, \tag{9}$$

which sets the neutralino energy scales relevant to our study: PeVs-EeVs for squarks and selectrons, and hundreds of ZeVs for *sneutrino* bursts.

The peak cross section $\sigma^{peak} \equiv \sigma(s = m_{\tilde{f}}^2)$ can be obtained from eq. (6) in a straightforward way :

$$\sigma^{peak} = \frac{8 \, \pi}{m_{\tilde{f}}^2} \, \left(\frac{m_{\tilde{f}}^2}{m_{\tilde{f}}^2 - m_\chi^2} \right)^2 \, B(\tilde{f} \to f \, \chi_1^0) \, B(\tilde{f} \to X). \tag{10}$$

In the final event-rate estimate, a crucial quantity will be given by the product $\sigma_{peak} \, \Gamma_{\tilde{f}}$, the resonance peak cross section times its total decay width (the latter setting the actual energy width of the resonance curve), that in general will depend on all the 5 mSUGRA parameters.

In this analysis, we will concentrate on some important scenarios where a relatively small parameter dependence is left in the cross sections, apart from the leading $m_{\tilde{f}}$ and m_χ mass dependence. In particular, in these (quite general) scenarios, there will be little parameter dependence in the $\tilde{f}$ decay branching fractions into both the initial $f\chi_1^0$ and final X states, these branching fractions being the crucial parameters entering σ_{peak}. These conditions most naturally realize in processes where the resonance is maximally coupled to the initial $f\chi_1^0$ state [that is $B(\tilde{f} \to f\ \chi_1^0) \simeq 1$], and, at the same time, one considers as decay products just the same initial $f\chi_1^0$ particles, in the process

$$\chi_1^0 + f \to \tilde{f} \to \chi_1^0 + f\ . \tag{11}$$

Then, the corresponding peak cross section becomes

$$\sigma^{peak} \to \frac{8\ \pi}{m_{\tilde{f}}^2}\ \left(\frac{m_{\tilde{f}}^2}{m_{\tilde{f}}^2 - m_\chi^2}\right)^2\ . \tag{12}$$

In the same scheme, also the parameter dependence of the total width $\Gamma_{\tilde{f}}$ will be mainly restricted to phase-space mass effects.

A natural framework were to implement the above picture is given by the *right selectron* and *right squark* resonances in mSUGRA. In mSUGRA, the right selectron $\tilde{e}_R$ is in general one of the lightest superpartner, and the lightest neutralino is mainly a bino $\tilde{B}$. For conserved R parity, the dominant $\tilde{e}_R$ decay channel is $\tilde{e}_R \to e\chi_1^0$, with a corresponding branching fraction of almost 100 %. On the other hand, the left selectron $\tilde{e}_L$ is usually more coupled to the second lightest neutralino χ_2^0 and to the lightest chargino χ_1^+. Hence, when allowed by phase-space, the decays $\tilde{e}_L \to \chi_2^0 e$ and $\tilde{e}_L \to \chi_1^+ e$ tend to be dominant. Therefore, $B(\tilde{e}_L \to e\ \chi_1^0)$ is in general not very large, and depletes the peak $e\ \chi_1^0 \to \tilde{e}_L \to X$ cross section.
On the other hand, for the right selectron, according to eq. (10), the peak cross-section is maximized when looking to at a $\chi_1^0 e$ final state in the channel

$$\chi_1^0 + e \to \tilde{e}_R \to \chi_1^0 + e\ , \tag{13}$$

being $m_{\tilde{e}_R}$ and m_χ the only relevant parameters that govern the cross section, as from eq. (12).

Then, the dominant signature of the resonant interaction of a neutralino with an electron in the detector will be an energetic electron carrying away a fair fraction of the initial neutralino resonant energy. *The $\tilde{e}_R$ signature will be totally characterized by an electromagnetic showering, while the Glashow W resonance will be mostly proceeding through hadronic channels.*

For the *squark* sector, that is relevant in the neutralino interactions with the nuclei of the detector, a similar discussion holds regarding the branching fractions of the right and left squarks into $q\chi_1^0$ [in particular, one has $B(\tilde{q}_R \to q\ \chi_1^0) \sim 1$, $B(\tilde{q}_L \to q\ \chi_1^\pm) \sim 2/3$, and $B(\tilde{q}_L \to q\ \chi_2^0) \sim 1/3$], unless the gluino is lighter than the squark. In the latter case, the strong interacting decay $\tilde{q}_{R,L} \to q\tilde{g}$ is by far dominant, and the effective squark coupling to the initial $q\tilde{\chi}_1^0$ is suppressed [due to the small branching fraction $B(\tilde{q} \to q\ \chi_1^0) \sim \Gamma(\tilde{q} \to q\ \chi_1^0)/\Gamma(\tilde{q} \to q\ \tilde{g})$]. However, (as noted above) σ_{peak} is not the only relevant quantity for event rates, since it enters the latter through the product $\sigma_{peak}\Gamma_{\tilde{q}_R}$ that also involves the total squark width. With the onset of the gluino decay channel, the decrease of $B(\tilde{q_R} \to q\ \chi_1^0)$ in eq. (10) is compensated by the corresponding increase in the total width $\Gamma_{\tilde{q}_R}$. Hence, when including the gluino decay $\tilde{q_R} \to q\,\tilde{g}$ into the *visible* final states of the process [hence keeping $B(\tilde{q}_R \to X) \sim 1$] the final event rate will be the same as in the case of the lighter-than-gluino squark.

In the following we will concentrate on the resonant production of *up* and *down* right squarks, $\tilde{u}_R$ and $\tilde{d}_R$, in the processes

$$\chi_1^0 + u, d \to \tilde{u}_R, \tilde{d}_R \to \chi_1^0 + u, d \,, \tag{14}$$

assuming $B(\tilde{u}_R, \tilde{d}_R \to \chi_1^0 + u, d) \simeq 1$. The dominant signature in the detector will then be given by a strongly interacting particle initiated shower, carrying some relevant fraction of the initial χ_1^0 energy.

4 Expected event rate at IceCube in mSUGRA benchmark scenarios

In mSUGRA with conserved R parity, the lightest neutralino is stable and provides an ideal candidate for explaining the origin of the cold dark matter (CDM). Taking into account the constraints on the CDM density obtained by combining the precise measurement of the cosmic microwave background by the WMAP experiment [31] and other cosmological data (that give $0.094 \leq \Omega_{CDM} h^2 \leq 0.129$ at 2-σ level), one should then require that the relic density of the lightest neutralino from primordial universe be compatible with $\Omega_{CDM} h^2$. In particular, requiring that most of the CDM is made up of lightest neutralinos restricts quite a lot the allowed region of the mSUGRA $(m_0, m_{1/2})$ parameter plane (see, e.g., [32], and references therein).

In [33], a set of 13 mSUGRA benchmark scenarios (characterized by a given set of values for the mSUGRA parameters m_0, $m_{1/2}$, A_0, at the GUT scale, and by the values of $\tan\beta$ and $sign\,\mu$) have been chosen, respecting the following experimental constraints: non-observation of SUSY partners at colliders (especially at LEP) [22, 23, 34]; bounds on deviation from the SM $b \to s\gamma$ decay rate; agreement of the lightest-neutralino relic density with $0.094 \leq \Omega_{CDM} h^2 \leq 0.129$.

Of the 13 benchmark points in [33], 5 points (B', C', G', I', L') are in the 'bulk' region (i.e. at moderate m_0, $m_{1/2}$ values), 4 points (A', D', H', J') are along the co-annihilation 'tail' (at moderate m_0 and larger $m_{1/2}$, where the neutralino-stau co-annihilation channel considerably affects the neutralino relic density), 2 points (K', M') are along rapid-annihilation 'funnel' (where both m_0 and $m_{1/2}$ can grow large with large $\tan\beta$), and 2 points (E', F') are in the 'focus-point' region, at very large m_0.

In the present analysis, the two crucial parameters ruling the signal rates are the resonance scalar mass $m_{\tilde{f}}$ and the splitting in the square of the scalar and neutralino masses, $m_{\tilde{f}}^2 - m_\chi^2$. Then, we found that scenarios like K', M' ('funnel') and E', F' ('focus points'), where the scalar mass parameter is quite large ($m_0 \geq 1$ TeV $\Rightarrow m_{\tilde{f}} > 1$ TeV), give rise to drastically reduced signals (less than 0.01 events/year in Icecube, see below). On the other hand, for such large scalar masses, t-channel diagrams in the $\chi_1^0 f$ scattering can become dominant over the resonant s-channel, in case neutralino has a non-negligible higgsino component (cf. 'focus-point' scenarios). Then, the approximation of restricting the cross section evaluation to the resonant channel (on which the present analysis in based) could fail. Hence, in our study, we will consider only the 'bulk' and co-annihilation benchmarks, leaving the analysis of the 'funnel' and 'focus-point' scenarios to a more complete treatment.

The 9 benchmark points we include in our analysis are reported in Table 1. They correspond either to the 'bulk' region (B, C, G, I, L) or to the co-annihilation region (A, D, H, J). In all scenarios, $A_0 = 0$.

Model	A	B	C	D	G	H	I	J	L
$m_{1/2}$ (GeV)	600	280	400	525	375	935	350	750	450
m_0 (GeV)	107	57	77	101	110	233	180	298	303
$\tan\beta$	5	10	10	10	20	20	35	35	47
sign(μ)	+	+	+	−	+	+	+	+	+
Ωh^2	0.128	0.123	0.122	0.116	0.110	0.123	0.117	0.119	0.113
m_χ (GeV)	243	107	158	212	148	388	138	309	181
$m_{\tilde{e}_R}$ (GeV)	254	128	175	226	184	423	227	412	349
$\Gamma_{\tilde{e}_R}$ (MeV)	9.13	57.2	29.7	16.3	103	53.4	448	396	931
$\sigma^{peak}_{\tilde{e}_R}$ (μb)	21.1	6.58	9.34	13.3	2.57	2.17	0.477	0.301	0.150
$\mathcal{N}_{\tilde{e}_R}$	28	32	26	23	8.5	2.3	1.9	0.55	0.42
(km^{-3} yr^{-1})	37	45	34	30	7.7	1.4	1.1	0.20	0.14
$m_{\tilde{q}_R}$ (GeV)	1194	596	825	1057	781	1798	748	1487	961
$\Gamma_{\tilde{q}_R}$ (GeV)	2.45	1.23	1.70	2.17	1.61	3.65	1.55	3.04	1.99
$\sigma^{peak}_{\tilde{q}_R}$ (nb)	7.43	28.6	15.3	9.46	17.1	3.32	18.5	4.81	11.3
$\mathcal{N}_{\tilde{q}_R}$	0.35	3.0	1.1	0.52	1.3	0.08	1.5	0.17	0.70
(km^{-3} yr^{-1})	0.22	2.6	0.89	0.36	1.1	0.04	1.2	0.09	0.51

Table 1: Definition of different mSUGRA scenarios and corresponding event-number expectations $\mathcal{N}_{\tilde{e}_R,\tilde{q}_R}$, for resonant neutralino scattering in ice. In all scenarios, we assume $A_0 = 0$. The resonance decay widths and peak cross sections for the right selectron and right squark are also shown. The upper of the two entries in the $\mathcal{N}_{\tilde{e}_R,\tilde{q}_R}$ raws corresponds to the event number calculated by the neutralino flux in eq. (4) ($\beta_0 = 1.5$), while the lower entry refers to eq. (5) ($\beta_0 = 2$). When computing the squark event rates, an incident neutralino energy threshold of 1 PeV is assumed. The relic DM density Ωh^2 corresponding to each scenario is also shown.

Starting from the values of m_0, $m_{1/2}$, A_0 at the GUT scale, and $\tan\beta$, $sign\,\mu$, all the physical masses and couplings of the spectrum of SUSY partners can be calculated at the electroweak scale by solving a set of renormalization group equations. There are many public spectrum calculators doing this task, including second-order radiative corrections (see, i.e., [35]). The differences in the corresponding results is considered a good estimate of the present theoretical uncertainty in the computation of SUSY spectra.
Then, the high precision of the WMAP $\Omega_{CDM}h^2$ determination (that slimmed considerably the allowed mSUGRA parameter regions) gives rise, through the prediction of the neutralino relic density versus mSUGRA parameters, to some sensitivity of the allowed mSUGRA regions to the choice of the spectrum calculator in the analysis. The differences in results is considered a good estimate of the present theoretical uncertainty of this kind of analysis.
The impact of the sensitivity to the details of the mSUGRA spectrum has been analyzed in [35] through the code micrOMEGAs 1.3 [36] that can evaluate the neutralino relic density assuming different codes for the mSUGRA spectrum. One finds that mass differences of about 1% in the mSUGRA spectrum can imply sometimes a 10% variation (and even larger for high $\tan\beta$ and m_0) in the corresponding neutralino relic density.

The above discussion motivates the choice of our benchmark points in Table 1. In our analysis, we used Isajet 7.71 [37] to compute the mSUGRA spectrum[5], and micrOMEGAs 1.3 to compute the corresponding neutralino relic density (as implemented in the last reference in

[5]In Isajet7.71, we set $m_b(m_b)^{\bar{MS}} = 4.214$ GeV, $\alpha_s(M_Z)^{\bar{MS}} = 0.1172$ and the top pole mass at $m_t = 175$ GeV.

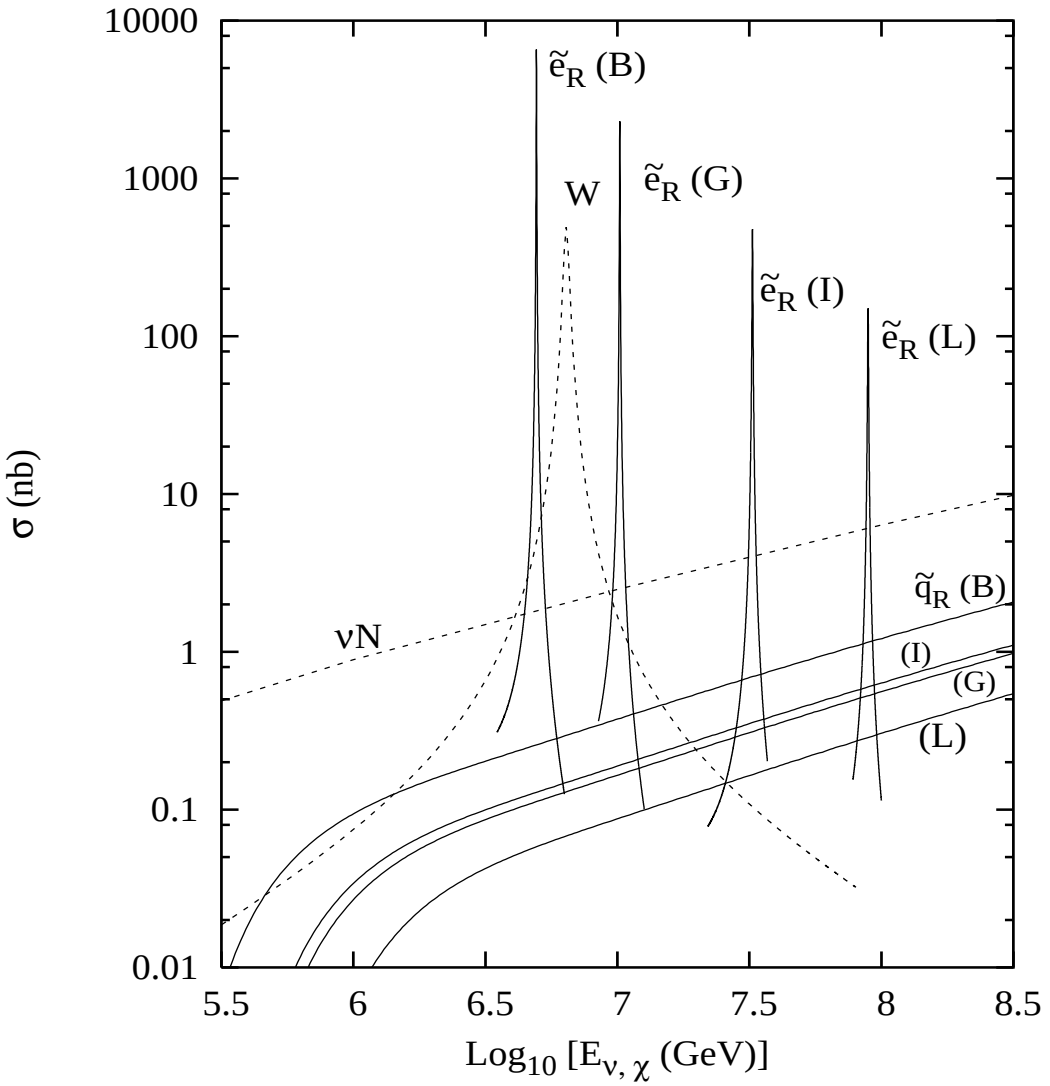

Figure 2: Cross sections (in nb) for the resonant right-selectron/right-squark production by UHE neutralino scattering on electrons/nucleons, in the four mSUGRA scenarios B, G, I, L defined in Table 1. For comparison, the dashed lines show the scattering cross sections of UHE anti-neutrinos on electrons (when marked by W) and nucleons (when marked by νN).

[35]). The small differences in the definition of our benchmarks A, B, C, ... in Table 1 with respect to the corresponding post-WMAP benchmarks A', B', C', ... defined in Table 2 of [33] (which are based on ISASUGRA 7.67) are due to the small adjustments in the choice of $m_{1/2}$ and m_0 needed to pass both the relic-density and LEP constraints by assuming a different code.

In Table 1, one can read the neutralino relic density, Ωh^2, corresponding to each scenario, that is well compatible with the assumption that the lightest neutralino be the main CDM component. For each benchmark, we show the lightest-neutralino, right-selectron and right-squark masses (masses for squark of different flavors u, d, s, c are assumed to be degenerate and equal to $m_{\tilde{q}_R}$). In all scenarios, one finds $m_{\tilde{e}_R} < 0.5$ TeV, and $m_{\tilde{q}_R} < m_{\tilde{g}}$, so that $B(\tilde{q}_R \to q\, \chi_1^0) \sim 1$. Total right-selectron and right-squark widths, $\Gamma_{\tilde{e}_R}$ and $\Gamma_{\tilde{q}_R}$ are also shown

in Table 1, along with the respective peak cross sections, $\sigma^{peak}_{\tilde{e}_R}$ and $\sigma^{peak}_{\tilde{q}_R}$, as defined in eq. (10) with $B(\tilde{f} \to X) \simeq B(\tilde{f} \to f\ \chi^0_1)$.

In Fig. 2, we show (for the B, G, I, L scenarios) the cross sections for the resonant production of a right selectron and a right squark from the UHE neutralinos scattering on electrons and nucleons, respectively, versus the incident neutralino energy.

For comparison, we also present the resonant neutrino cross section for $\bar{\nu}_e e^- \to W^- \to all$, and the (non-resonant) neutrino-nucleon cross section. Indeed, a Breit-Wigner W peak cross section is expected at the incident neutrino energy (E_ν)

$$E^{peak}_\nu = \frac{M^2_W - m^2_\nu}{2m_e} \simeq \frac{M^2_W}{2m_e} \sim\ 6.3 \times 10^6\ \mathrm{GeV}\ , \tag{15}$$

although present observation of UHE energy neutrino events does not reach such energies yet.

Cross sections for the resonant squark production do not show the Breit-Wigner structure. Because of the continuous quark momentum distribution inside a nucleon N, any value of the incident neutralino energy larger than a threshold ($E_\chi > \frac{m^2_{\tilde{q}} - m^2_\chi}{2m_N}$, where m_N is the nucleon mass) can produce a squark at resonance. In this case, the cross section evaluation involves a convolution of the partonic cross section in eq. (6) (with $f \equiv u, d$ and *sea* quarks) with a parton distribution function $f_q(x, Q^2)$, where x is the momentum fraction of the proton carried by the parton, and Q is the energy scale at which we evaluate this distribution. In our computation, we used the CTEQ4L set of structure functions in [38].

The $\tilde{u}_R$ and $\tilde{d}_R$ decay widths are small compared to their masses, and one can substitute the Breit-Wigner propagator in the partonic cross section by a δ-function. Then, the squark-resonance cross section in the χ^0_1-nucleon scattering becomes:

$$\sigma_{\tilde{q}_R}(E_\chi) = \pi\ \sum_q\ \frac{\sigma^{peak}_{\tilde{q}_R}\ \Gamma_{\tilde{q}_R}}{m_{\tilde{q}_R}}\quad x_q\ \ f_q(x_q, m^2_{\tilde{q}_R}) \tag{16}$$

where, $x_q = m^2_{\tilde{q}_R}/(m^2_{\chi^0_1} + 2\ E_\chi m_N)$. The summation in eq. (16) is over the u- and d-type quarks (thus including also s and c quarks) in an isoscalar target. In our scenarios, one has $m_{\tilde{u}_R} \simeq m_{\tilde{d}_R} \simeq m_{\tilde{c}_R} \simeq m_{\tilde{s}_R}$ and $\Gamma_{\tilde{u}_R} \simeq \Gamma_{\tilde{c}_R} \simeq 4\ \Gamma_{\tilde{d}_R} \simeq 4\ \Gamma_{\tilde{s}_R}$.

The actual event rates $\mathcal{N}_{\tilde{f}}$ can be calculated from the cross section by convoluting it with the appropriate neutralino flux, and multiplying the result by the number of the target electrons/nucleons $\mathcal{N}_T$ in a given detector volume, and by the exposure time Δt, as follows

$$\mathcal{N}_{\tilde{f}} = \mathcal{N}_T\ \Delta t\ \int \sigma_{\tilde{f}}(E_\chi)\ \frac{dN}{dE_\chi}\ dE_\chi\ . \tag{17}$$

For selectrons and squarks $\sigma_{\tilde{f}}(E_\chi)$ will be given by eq. (6) and eq. (16), respectively. We assumed the two different neutralino fluxes in eq. (4) and eq. (5). $\mathcal{N}_T$ is given by the product of the detector mass (in g units) and Avogadro number (N_A) for nucleons (times 11/18 for electrons).

The selectron width being small compared to its mass (see Table 1), we approximated the Breit-Wigner propagator in eq. (6) by a δ-function. The corresponding expected event number is then

$$\mathcal{N}_{\tilde{e}_R} = \alpha_{\tilde{e}_R}\ \sigma^{peak}_{\tilde{e}_R}\ \Gamma_{\tilde{e}_R}\ \left(\frac{m_{\tilde{e}_R}}{2\ m_e}\right)\left(E^{peak}_\chi\right)^{-\beta_0}\ , \tag{18}$$

where the factor $\alpha_{\tilde{e}_R}$ (depending on the mass of the detector, exposure time and nature of the neutralino flux) includes the product of Δt, $\mathcal{N}_T$, and the normalization of the fluxes defined in

eq. (4) and eq. (5). The exponent β_0 sets the shape of the neutralino flux, and is equal to 1.5 and 2, respectively, for the two cases, while E_χ^{peak}, expressed in GeV, is given by eq. (9) where $f \to e$.

For an ice detector of 1 km^3 and one year of exposure, one has $\alpha_{\tilde{e}_R} = 7.24 \times 10^3$ [2.29×10^7] nb^{-1} GeV$^{\beta_0 - 1}$ for the flux in eq. (4) [eq. (5)]. The large difference in the α factors is an artifact due to the exponent β_0 in the formula above.

Number of events from UHE ν, $\bar{\nu}$ interaction		
$W^- \to e\bar{\nu}_e$	$W^- \to$ hadrons	$\sum_i (\nu_i + \bar{\nu}_i)_{CC+NC}$
2	12	55
2.5	15	56

Table 2: Number of events from UHE neutrino/antineutrino CC and NC interaction in IceCube per year. In each entry, the upper number refers to the flux in eq. (4) ($\beta_0 = 1.5$) for the $\nu_i + \bar{\nu}_i$ spectrum, while the lower number assumes the flux in eq. (5) ($\beta_0 = 2$). An incident-neutrino energy threshold of 1 PeV is used.

For the $\tilde{q}_R$-resonances, due to the energy distribution of the partons in a nucleon, the number of events will get contributions from a continuous range of incident neutralino energies

$$\mathcal{N}_{\tilde{q}_R} = \alpha_{\tilde{q}} \int_{E_\chi^{min}} \sigma_{\tilde{q}_R}(E_\chi) \; E_\chi^{-\beta_0} \; dE_\chi \; , \tag{19}$$

where, for a 1-km^3 ice detector and one year of exposure, $\alpha_{\tilde{q}_R} = 3.77 \times 10^3$ [1.19×10^7] nb^{-1} GeV$^{\beta_0 - 1}$ for the flux in eq. (4) [eq. (5)], and $\sigma_{\tilde{q}_R}(E_\chi)$ is given by eq. (16).

One can note that the peak cross section in eq. (12) is enhanced for small mass differences between the selectron/squark and the neutralino. However, in the product $\sigma_{\tilde{f}}^{peak} \, \Gamma_{\tilde{f}}$ that enters the event numbers in eq. (18), and in eq. (19) through eq. (16), the $1/(m_{\tilde{f}}^2 - m_\chi^2)^2$ behavior in $\sigma_{\tilde{f}}^{peak}$ is compensated by the resonance-width, that goes as $(m_{\tilde{f}}^2 - m_\chi^2)^2$. On the other hand, a residual enhancement associated to the resonance-neutralino mass degeneracy arises from the factor $\left(E_\chi^{peak}\right)^{-\beta_0}$ in eq. (18) (cf. eq. (9)), and from the lower limit $E_\chi^{min} = (m_{\tilde{q}}^2 - m_\chi^2)/(2m_N)$ of the integral in eq. (19). Hence, selectrons/squarks and neutralinos that are closer in mass tend to increase the expected event number.

In Table 1, we present the number of events ($\mathcal{N}_{\tilde{e}_R,\, \tilde{q}_R}$), per km^3 per year, expected in an ice detector for the different mSUGRA benchmarks. The number $\mathcal{N}_{\tilde{q}_R}$ was always worked out by assuming as lower limit in the integration in eq. (19) the value $E_\chi^{min} \simeq 10^6$ GeV in order to cut off the atmospheric neutrino pollution. In Table 1, the raws corresponding to the number of events have two entries. The upper one corresponds to the neutralino flux defined in eq. (4) ($\beta_0 = 1.5$), while the lower one assumes the flux in eq. (5) ($\beta_0 = 2$).

For comparison, the expected event rates for the resonant W production from $\bar{\nu}_e e$ scattering, in the hadronic and leptonic channels, are presented in Table 2. Since the fluxes in eqs. (4) and (5) are relative to one flavor of $\nu + \bar{\nu}$, assuming a complete neutrino flavor mixing due to non-zero neutrino masses, in Table 2 we use a $\bar{\nu}_e$ flux that is half of those defined in eq.(4) and eq.(5). We also show total ν-N and $\bar{\nu}$-N charged-current (CC) plus neutral-current (NC) event rates.

In scenarios A, B, C, D, where one has both a light selectron ($m_{\tilde{e}_R} \lesssim 250$ GeV) and quite degenerate $m_{\tilde{e}_R}/m_\chi$ values, one obtains in IceCube a few tens of events per year in the electronic

channel. Note that the selectron/neutralino degeneracy favors $\mathcal{N}_{\tilde{e}_R}$ in the harder-spectrum case with $\beta_0 = 1.5$. In scenarios H, I, J, L the larger splitting in $m_{\tilde{e}_R}$ and m_χ, and the quite heavy selectron deplete the event rates by more then one order of magnitude (0.2-2 events per year). Note that in this case the $\beta_0 = 2$ spectrum gives higher $\mathcal{N}_{\tilde{e}_R}$. The benchmark G shows an intermediate case, where the selectron is quite light, while $m_{\tilde{e}_R}$ and m_χ are not much degenerate, giving rise to about 8 events per year.

Concerning the hadronic channel, due to the large squark masses ($m_{\tilde{q}_R} \gtrsim 600$ GeV) and their large splitting with m_χ, the signal is modest in all benchmarks, reaching the level of 1-3 events per year only in the B, C, G, I points.

With the assumed neutralino fluxes, one could expect a clear SUSY signal in IceCube in the electronic channel for most of the analyzed benchmarks. Only scenarios J and L foresee less than 1 event per year in both the electronic and hadronic channel. We recall that the normalization of the fluxes in eqs. (4) and (5) is quite conservative. Due to the lower neutralino-nucleon cross section $\sigma_{\chi N} \lesssim \frac{1}{10}\sigma_{\nu N}$ (cf. Fig. 2), one is presently allowed to assume flux normalizations that are an order of magnitude larger than the ones adopted here without violating any experimental constraint. This would make the event statistics even more promising.

5 Disentangling the neutralino signal by neutrino calibration

We will now briefly address the problem of the effective *visible-energy* spectrum coming from the two body decays $\tilde{f}_R \to f\chi_1^0$, that is of course a crucial characteristic in the detection of a resonance signal.

In the resonant $\tilde{e}_R$ decay into an electron plus an invisible neutralino χ_1^0, only the electron energy contributes to the visible energy. In Fig. 3, we plot the visible-energy spectrum $\Delta z \frac{dN}{dz}$ (where $z = \log_{10} E_{vis}$, and $\Delta z = 0.1$ assumes a 10% experimental resolution) corresponding to the resonant $\tilde{e}_R$ production and decay into $e\chi_1^0$, for benchmarks A, B, G, I. The positions of the sharp end-points of the spectra are determined by the resonance and neutralino masses. For comparison, we also show the expected visible-energy spectrum for a resonant W decaying into either $e\nu$ or hadrons. When the W decays hadronically, the total energy of the initial incident neutrino gives rise to visible energy in the final state. In this case, the $\Delta z \frac{dN}{dz}$ spectrum has a resonant structure corresponding to the initial neutrino energy $E_\nu \simeq m_W^2/(2m_e) \simeq 6.3 \times 10^6$ GeV. When the W decays leptonically, only a fraction of the incident neutrino energy goes into visible energy, whose distribution is characteristic of a two-body decay, just as in $\tilde{e}_R \to e\chi_1^0$. The different positions of the spectrum end-points could then provide a handle to disentangle the visible energy of the $\tilde{e}_R$ decay from the one of the W decay.

The hadronic W^- decay defines a sharply clustered group of events [about 12 for the $\beta_0 = 1.5$ spectrum, and 15 for the $\beta_0 = 2$ power law, per year, cf. Table 2], whose intensity may be correlated with the two electromagnetic channels arising from $W^- \to e^- + \bar{\nu}_e$ [2 and 2.5 events] and $W^- \to \tau^- + \bar{\nu}_\tau$ [2 and 2.5 events]. The channel $W^- \to \mu^- + \bar{\nu}_\mu$ [2 and 2.5 events] is delivering just a single PeV muon track, that is quite difficult to recognize. The electron and tau electromagnetic energy spectra grow linearly with energy up to $E = 6.3$ PeV, and their average energy is about half of the hadronic-channel energy. The distribution is spread according to a continuous power law, as shown in Fig. 3. The τ birth and decay will be in

general source of a characteristic *double-bang* event [39].

In conclusion, the appearance of a sharp edge at some energy different from the expected W^- hadronic, electronic, and tau bumps could point to some new physics corresponding to the resonant $\tilde{e}_R$ production from UHECR neutralinos. Such reconstruction seems possible for a neutralino flux that is comparable to (and, in favorable scenarios, even lower than) the present lower bounds on neutrino fluxes.

The mass ranges considered are of great astrophysical interest, and within the reach of the CERN LHC. A near-future underground ν-detector could then cross-check a possible SUSY discovery at future colliders.

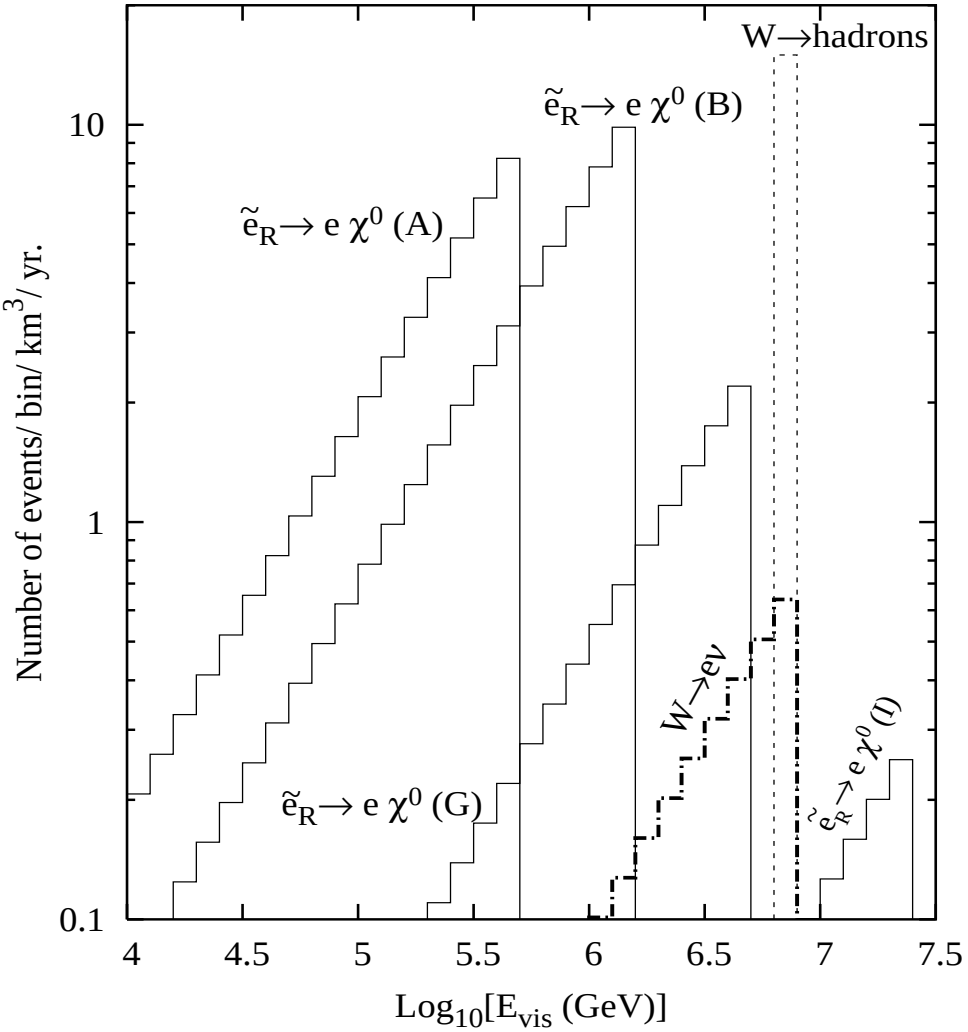

Figure 3: Visible energy spectra of the resonance decay products [assuming the flux in eq. (4) ($\beta_0 = 1.5$)]. For the resonant W production and decay, the dash-dotted (dashed) histogram represents the electron (hadronic) energy spectrum in the lab. The four solid-line distributions refer to the electron energy spectra arising from $\tilde{e}_R \to e\chi^0$ in the mSUGRA scenarios A, B, G, I defined in Table 1.

6 The role of the sneutrino burst

The resonant production of Z-bosons via UHE ν scattering off massive relic neutrinos has been the backbone of the so called *Z-burst* mechanism [16] that could explain the GZK puzzle. UHE neutrinos in *Z-burst* are the messengers able to overcome the GZK cut-off, by offering a link between UHECR and most distant cosmic sources. About 70% of the $Z-$bosons decays hadronically, thus producing protons, neutrons and anti-nucleons as well as pions (and consequent photons from neutral-pions decays). The Z-decay products could have quite naturally energies beyond the GZK scale for appropriate relic-neutrino masses, since $E_\nu \simeq M_Z^2/(2m_\nu) \simeq 4 \cdot 10^{22} \left(\frac{0.1eV}{m_\nu}\right) eV$, which corresponds to a UHECR proton energy of $E_p \simeq \frac{1}{20} \cdot M_Z^2/(2m_\nu)$. If relic-neutrino halos are present at distances less than about 50 Mpc [6], then these protons or anti-protons (or photons) could arrive to the earth atmosphere without much energy loss. Consequently, air-showers produced by these extremely high-energy nucleons could give rise to the *super* GZK events, as detected by the AGASA experiment [3]. Crucial ingredients of this picture are of course sufficiently large UHE-neutrino fluxes and relic-neutrino densities in the Local Group or Super Galactic Plane. Then, the *Z-burst* model has a good potential for explaining observed correlation of UHECR arrivals from BL-Lac sources at distances well above GZK, and electron pair losses [5].

In this section, we will consider the resonant sneutrino ($\tilde{\nu}$) production from the UHE neutralinos scattering off relic neutrinos, and its subsequent decay into visible final states

$$\chi_1^0 \nu \to \tilde{\nu} \to X_{vis} \ , \tag{20}$$

where X_{vis} stands for the all final states with at least one visible particle. In particular, we will discuss whether this process can have a role similar to the *Z-burst* in the observed component of the cosmic-ray spectrum beyond the GZK energy.

The channel in eq. (20) differs from the previously analyzed resonant selectron and squark production under various aspects. First, due to the lightness of the target ν mass, it requires much larger χ_1^0 energies according to eq. (9). Second, optimizing cross sections by considering scenarios where the sneutrino is maximally coupled to the initial state, and, at the same time, it decays into the initial particles $\tilde{\nu} \to \chi_1^0 \nu$ is not viable, since this would give rise to invisible final states. On the other hand, the sneutrino can decay into heavier neutralinos χ_i^0 $(i = 2, 3, 4)$ and charginos $\chi_j^\pm$ $(j = 1, 2)$. The subsequent neutralino and chargino decays into hadrons and leptons might produce highly energetic protons, pions and electrons that would be able to initiate the super GZK air showers. Looking back at eq. (6) for the cross section, one is interested in scenarios where neither $B(\tilde{\nu} \to \chi_1^0 \nu)$ nor $B(\tilde{\nu} \to X_{vis})$ are small. The latter are complementary quantities, since one can assume quite accurately $B(\tilde{\nu} \to X_{vis}) \simeq 1 - B(\tilde{\nu} \to \chi_1^0 \nu)$. Hence, the sneutrino production cross section is automatically penalized. Furthermore, the rates will be in general quite model dependent. Our results will not be simply determined by the particle mass spectrum (as in the right selectrons/squarks production), but will depend also on couplings (and on the $\tan\beta$ and μ parameters) in a nontrivial way. Finally, since a visible sneutrino channel will arise from a decay chain, the energy of the visible decay products can in principle be quite depleted. In the following, we will also discuss the sneutrino energy flow in the visible decay products.

[6] The distances of the center of dense clusters from the earth are estimated to be 16 Mpc for Virgo, while our Super-Galactic Plane diameter is about 50 Mpc [40].

Model	I	L
$m_{1/2}$ (GeV)	350	450
m_0 (GeV)	180	303
$\tan\beta$	35	47
sign(μ)	+	+
Ωh^2	0.117	0.113
$m_{\tilde{\nu}}$ (GeV)	291	424
$m_{\chi_1^0}$ (GeV)	138	181
$m_{\chi_2^0}$ (GeV)	265	350
$m_{\chi_1^\pm}$ (GeV)	266	350
$\Gamma_{\tilde{\nu}}$ (MeV)	329	885
$B_{\chi_1^0}$ (GeV)	0.71	0.42
$B_{\chi_2^0}$ (GeV)	0.09	0.19
$B_{\chi_1^\pm}$ (GeV)	0.20	0.39
$\sigma_{\tilde{\nu}}^{peak}$ (nb)	39.4	19.8
$\sigma_{\tilde{\nu}}^{peak}\Gamma_{\tilde{\nu}}$ (nb GeV)	13.0	17.5

Table 3: Relevant mass spectra, widths, branching fractions and peak cross sections for the resonant sneutrino scattering, in the two mSUGRA scenarios I, L defined in Table 1.

The sneutrino branching fraction into visible final states $B(\tilde{\nu} \to X_{vis})$ is in general made up of different components

$$B(\tilde{\nu} \to X_{vis}) \equiv \sum_{j=1}^{2} B(\tilde{\nu} \to l\chi_j^\pm) + \sum_{i=2}^{4} B(\tilde{\nu} \to \nu\chi_i^0)\, B(\chi_i^0 \to f\bar{f}\chi_1^0) \sim 1 - B(\tilde{\nu} \to \chi_1^0\nu) \quad (21)$$

where $f \neq \nu$.

The $\tilde{\nu}$ decays into the second neutralino χ_2^0 and into the lightest chargino $\chi_1^\pm$, when allowed by phase space, are in general dominant. The subsequent decays $\chi_1^\pm \to q\bar{q}'\chi_1^0$ (with a branching ratio of about 66 %) and $\chi_1^\pm \to l\nu_l\chi_1^0$ (with a branching ratio of about 33 %) are the sources of hadrons and charged leptons, respectively, that may trigger the highest-energy air showers. The second neutralino can have a substantial decay rate into the invisible channel $\chi_2^0 \to \nu\bar{\nu}\chi_1^0$. Otherwise, a χ_2^0 decay produces quarks and leptons via $\chi_2^0 \to q\bar{q}\chi_1^0$, $l\bar{l}\chi_1^0$. The $\chi_2^0 \to e\tilde{e}_R$ decay may also be kinematically allowed. In the latter case, no hadron would arise from the decay chain.

The presence of a heavy invisible particle (χ_1^0) among the $\tilde{\nu}$ decay products makes the visible part of the spectrum quite different from the *Z-burst* case. The results are in general model dependent and less promising, and the incoming UHE χ^0 energy should be at higher energies. The decay kinematics of a *Z-burst* event is quite simple. The hadrons resulting from the $Z \to q\bar{q}$ decay carry away all the energy of the incident UHE neutrino (i.e., the Z resonance energy). On the other hand, the average energy of the visible sneutrino decay products is lower than the sneutrino mass, since hadrons can only appear either from a three-body decay of $\chi_2^0, \chi_1^\pm$, or from a two-body decay chain [$\chi_2^0(\chi_1^\pm) \to Z(W)\chi_1^0$, with $Z(W) \to$ hadrons] following the initial two-body $\tilde{\nu}$ decay. Sneutrino masses, anyway, can be quite heavier than the Z mass, and this could compensate partly the depletion of the average energy of the sneutrino decay products, that in any case would have a less *resonant* structure than in the *Z-burst* case. The detailed

energy spectrum of the hadrons and leptons coming from the sneutrino decay cascades also depends crucially on the masses of the particles in each step of the decay chains. Their study would require a Monte Carlo treatment of the complete kinematics. We will not go into this analysis here.

The observed event number is ruled by the product $\sigma_{\tilde{\nu}}^{peak}\Gamma_{\tilde{\nu}}$, that is the peak cross section (depending on the sneutrino branching fractions into the initial and final states) times the resonance width.

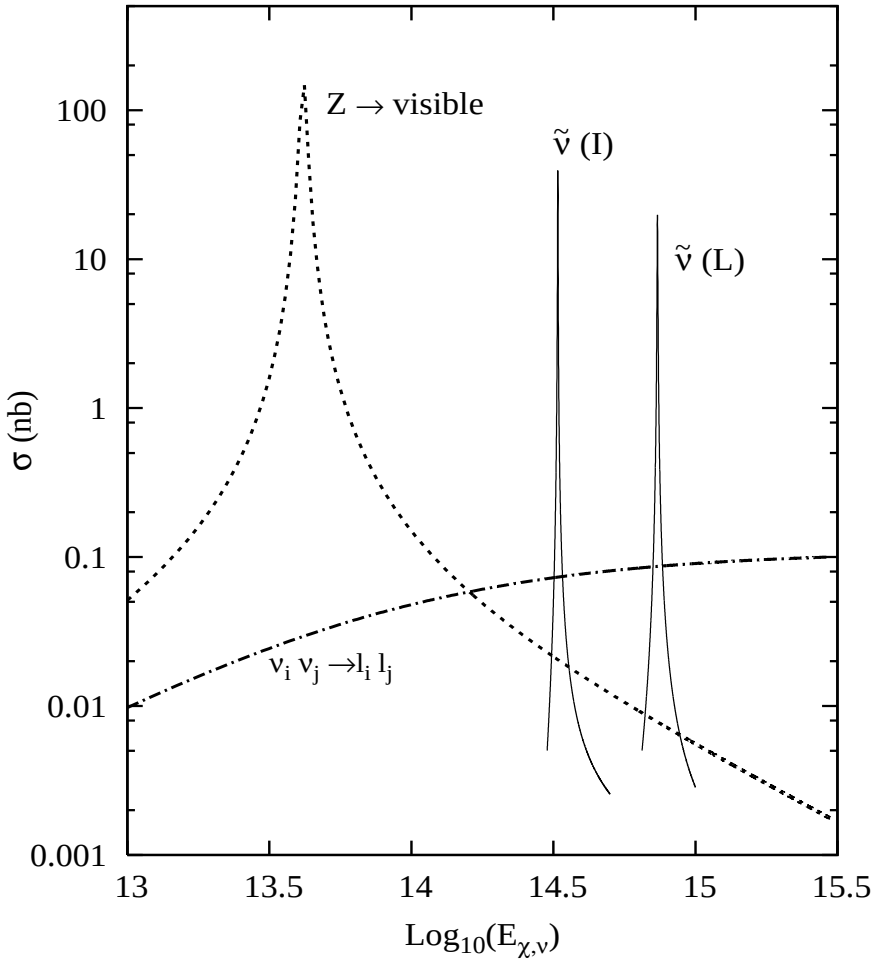

Figure 4: Cross sections (in nb) for resonant sneutrino production and visible decay (solid curves) coming from UHE neutralino scattering off relic neutrinos in the two mSUGRA scenarios I, L defined in Table 1. The dotted line represents the resonant Z-boson cross section for the scattering of UHE neutrinos off relic neutrinos. The dot-dashed line refers to the continuum cross section for $\nu_i\bar{\nu}_j^{relic} \to l_i\bar{l}_j$. We assumed a relic-neutrino mass $m_\nu = 0.1$ eV.

In Table 3, we present these quantities, along with the relevant mass spectrum and branching fractions, for the scenarios I and L, that are the only benchmarks among the ones presented in Table 1 for which sneutrino *visible* decays are allowed by phase space. In particular, sneutrino decay into the lightest chargino and second lightest neutralino (that are almost degenerate

in mass) are open. The sneutrino decay into heavier charginos and $\chi^0_{3,4}$ neutralinos are not allowed, which is important in order not to deplete too much $B(\tilde{\nu} \to \chi^0_1 \nu)$ and, as a consequence, the sneutrino cross section.

In Fig. 4, we plot the cross sections for the resonant $\tilde{\nu}$ production in the channel in eq. (20) versus the incident neutralino energy, for the scenarios I and L. The cross section for the Z-production from UHE-ν scattering off relic neutrinos is also shown versus the incident neutrino energy, for comparison. A relic neutrino mass of 0.1 eV is assumed in all cases [41] and the resonant incoming UHE neutralino energy is given by $E_\chi^{peak} \simeq (m^2_{\tilde{\nu}} - m^2_\chi)/(2m_\nu)$.

Both the sneutrino peak cross section and the sneutrino width in scenarios I and L are quite smaller than (although not very far from, cf. Table 3) the corresponding Z quantities, which are $\sigma_Z^{peak} \simeq 185$ nb and $\Gamma_Z \simeq 2.5$ GeV. In particular, one gets $\sigma_{\tilde{\nu}}^{peak} \cdot \Gamma_{\tilde{\nu}} \simeq 13 - 18$ nb GeV, to be compared with $\sigma_Z^{peak} \cdot \Gamma_Z \simeq 463$ nb GeV.

Of course, the latter comparison assumes a comparable flux of incident neutrinos and neutralinos. With this hypothesis, the *Z-burst* is expected to be dominant on the *sneutrino-burst*. Nevertheless, an extra fraction of sneutrino events could add to the *Z-burst* counting, presumably with a bit less structured energy distribution. Further in-depth analysis are needed to establish the latter point.

Note that, while calculating the peak cross sections, in both the Z and $\tilde{\nu}$ cases the relic light neutrinos are assumed to be Dirac fermions. In case of Majorana neutrinos, the peak cross sections are enhanced by a factor 2, doubling the number of the events in each case.

7 Conclusions

If elementary-particle interactions are governed by supersymmetry, then an important component of the UHECR may be given by the lightest stable supersymmetric particle, namely the lightest neutralino. For instance, some of the models trying to explain the UHECR spectrum beyond the GZK cut-off via super-heavy particle decays, when including supersymmetry, predict a flux of UHE neutralinos arriving to the earth. One of the major challenges of the future cosmic-ray experiments is to verify such predictions.

In this paper, we computed the event rates for right selectrons and right squarks produced on resonance, when UHE neutralinos scatter off the electrons and quarks in a detector like IceCube. We assumed a well-motivated model of supersymmetry, that is minimal supergravity, and analyzed the signal for moderate scalar masses, when the resonant scattering is expected to be dominant on the t-channel scattering.

The right scalar sector turns out to be particularly straightforward to analyze. One has in general $B(\tilde{e}_R \to e\ \chi^0_1) \simeq 1$, and $B(\tilde{q}_R \to q\ \chi^0_1) \simeq 1$. As a consequence, after constraining the mSUGRA parameter space by negative collider searches and neutralino relic-density bounds, the relevant phenomenology depends only on the physical masses of the resonant right scalar and lightest neutralino. Any other parameter dependence, such as the one arising from the neutralino physical compositions and couplings, drops off. We performed a detailed study in scenarios inspired to the post-WMAP mSUGRA benchmarks of [33].

For comparison, event rates for the expected resonant W signal in UHE anti-neutrino scattering off electrons in matter were also presented.

Two different phenomenological forms for the neutralino fluxes were assumed to calculate the event rates: power laws with exponent either $\beta_0 = 1.5$ or $\beta_0 = 2$. We set the flux normalization on the basis of present bounds on the UHE neutrino flux from the AGASA and

Fly's Eye experiments (assuming, quite conservatively, that interaction rates of neutrino and neutralino with matter are of comparable strength).

For similar neutrino and neutralino fluxes, in the leptonic channel the event rates for SUSY particle resonances are very promising (up to a few tens of events per year in IceCube). They are remarkably greater than the leptonic Glashow W signal for most of the post-WMAP benchmarks characterized by moderate scalar masses ($m_{\tilde{e}_R} \lesssim 500$ GeV), that fall either into the 'bulk' or into the co-annihilation region. The corresponding hadronic signal is less structured in the energy spectrum, and penalized by the larger resonance masses ($m_{\tilde{q}_R} \gtrsim 600$ GeV). A few events per year in Icecube are expected in the most promising benchmarks, in the hadronic case. Signal in the 'funnel' and 'focus point' benchmarks is depleted by the large m_0 down to less than 0.01 event/year.

We showed here for the first time the detailed spectrum of the visible energy released in the $\bar{\nu}_e e^-$ reaction in underground detectors, and discussed how to calibrate the SUSY signal through the expected W spectrum.

We also considered the possibility of resonant production of sneutrinos in the interaction of UHE neutralinos with light relic neutrinos in the extended Galactic or Local Group hot neutrino halo. The visible decay products of the sneutrinos might trigger air-showers beyond GZK energies, thus mimicking the so called *Z-burst* process. However, even in the most promising scenarios, we found that the *sneutrino-burst* event rate would be more than one order of magnitude smaller than the *Z-burst* rate (assuming similar fluxes for UHE neutrinos and neutralinos). Furthermore, the UHE neutralino energies tuned for the *sneutrino-burst* are usually higher than for neutrinos in *Z-burst*, making it less attractive than the standard *Z-burst* model.

In conclusion, we found a well-defined and interesting window of mSUGRA parameters that can be tested by the next-generation underground detectors. The corresponding signal may exceed in some cases the standard neutrino ones. Its imprint may be disentangled in a realistic way. These high-energy astrophysical traces could offer a new opportunity to high-energy astrophysics to anticipate SUSY discovery at colliders.

Acknowledgments

This work was partially supported by the RTN European Programme MRTN-CT-2004-503369 (Quest for Unification).

References

[1] K. Greisen, Phys. Rev. Lett. **16** 748 (1966) ; G. Zatsepin, V. Kuzmin, *Pisma Zh. Eksp. Teor. Fiz.* **4** 114 (1966) [*JETP Lett.* **4** 78 (1966)].

[2] Fly's Eye Collab., D. Bird et al., Astrophys. J. **441** 144 (1995).

[3] AGASA Collab., H. Hayashida et al., Astropart. Phys. **10** 303 (1999).

[4] A. Zech for the Hires Collab., astro–ph/0409140 .

[5] D. Gorbunov, P. Tinyakov, I. Tkachev and S. Troitsky, Astrophys. J. **577** L93 (2002); D. Fargion, A.Colaiuda, astro-ph/0409022.

[6] For a comprehensive review see, P. Bhattacharjee, G. Sigl, Phys. Rept.**327**, 109 (2000).

[7] L. Anchordoqui, T. Paul, S. Reucroft and J. Swain, Int. J. Mod. Phys. **A18** 2229 (2003); D. Torres, L. Anchordoqui, astro–ph/0402371 and references therein.

[8] C. T. Hill, Nucl. Phys. B **224**, 469 (1983); C. T. Hill, D. N. Schramm and T. P. Walker, Phys. Rev. D **36**, 1007 (1987); P. Bhattacharjee, C. T. Hill and D. N. Schramm, Phys. Rev. Lett. **69**, 567 (1992); V. Berezinsky, X. Martin and A. Vilenkin, Phys. Rev. D **56**, 2024 (1997); L. Masperi and G. A. Silva, Astropart. Phys. **8**, 173 (1998); L. Masperi and M. Orsaria, Astropart. Phys. **16**, 411 (2002); V. Berezinsky and A. Vilenkin, Phys. Rev. Lett. **79**, 5202 (1997); V. Berezinsky, M. Kachelriess and A. Vilenkin, Phys. Rev. Lett. **79**, 4302 (1997); V. A. Kuzmin and V. A. Rubakov, Phys. Atom. Nucl. **61**, 1028 (1998) [Yad. Fiz. **61**, 1122 (1998)]; P. Jaikumar and A. Mazumdar, Phys. Rev. Lett. **90**, 191301 (2003); M. Birkel and S. Sarkar, Astropart. Phys. **9**, 297 (1998); Z. Fodor and S. D. Katz, Phys. Rev. Lett. **86**, 3224 (2001); C. Coriano, A. E. Faraggi and M. Plumacher, Nucl. Phys. B **614**, 233 (2001).

[9] V. Berezinsky, M. Kachelriess, Phys. Lett. **B422** 162 (1998).

[10] V. Berezinsky, M. Kachelriess, Phys. Lett. **B434** 61 (1998); V. Berezinsky, M. Kachelriess Phys. Rev. **D63** 034007 (2001); V. Berezinsky, M. Kachelriess and S. Ostapchenko, Phys. Rev. **D65** 083004 (2002); R. Aloisio, V. Berezinsky and M. Kachelriess, Phys. Rev. **D64** 094023 (2004).

[11] S. Sarkar and R. Toldra, Nucl. Phys. **B621** 495 (2002); A. Ibarra, R. Toldra, Jour. High Energy Phys. **0206:006** (2002) .

[12] C. Barbot, M. Drees, Phys. Lett. **B533** 107 (2002); C.Barbot, M. Drees, Astrop. Phys. 20;5-44, 2003; C. Barbot, M. Drees, F. Halzen and D.Hooper, Phys. Lett. **B563** 132 (2003); C. Barbot, hep–ph/0308028.

[13] V. Dubrovich, D. Fargion, and M. Khlopov, hep–ph/0312105.

[14] For a review, see H. E. Haber and G. L. Kane, Phys. Rept. **117**, 75 (1985).

[15] For a recent review, see B. Mele, hep–ph/0407204.

[16] D. Fargion, B. Mele and A. Salis, Astrophys. J. **517** 725 (1999); T. Weiler, Astropart. Phys. **11** 303 (1999).

[17] L. Anchordoqui, H. Goldberg and P. Nath, Phys. Rev. **D70** 025014 (2004).

[18] O. Catalano, Nuovo. Cim. **24C** 445 (2001); L. Scarsi, Nuovo. Cim. **24C** 471 (2001).

[19] D. Fargion, Astrophys. J. **570** 909 (2002).

[20] D. Fargion, P. De Sanctis Lucentini, M. De Santis and M. Grossi, Astrophys. J. **613** 1285 (2004).

[21] See for example, J. Alvarez-Muniz and F. Halzen, AIP Conf. Proc. **579**, 305 (2001); astro–ph/0102106.

[22] LEP2 SUSY Working Group, *Combined LEP Selectron/Smuon/Stau Results, 183-208 GeV,* ALEPH, DELPHI, L3, OPAL Experiments, LEPSUSYWG/04-01.1 .

[23] T. Affolder et al., The CDF Collab., Phys. Rev. Lett. **88**, 041801 (2002).

[24] S.L. Glashow, Phys. Rev. **118**, 316 (1960).

[25] D. Fargion, M. Grossi, P. G. De Sanctis Lucentini and C. Di Troia, J. Phys. Soc. Jap. Suppl. **70B**, 46 (2001) [arXiv:hep-ph/0108050].

[26] A. Chamseddine, H. Arnowitt and P. Nath, Phys. Rev. Lett. **49** 970 (1982) ; R. Barbieri, S. Ferrara and C. Savoy, Phys. Lett. **B119** 343 (1982); L. Hall, J. Lykken and S. Winberg, Phys. Rev. **D27** 2359 (1983); A. Chamseddine, H. Arnowitt and P. Nath, Nucl. Phys. **B227** 121 (1983); N. Ohta, Prog. Theor. Phys. **70**, 542 (1983).

[27] J. Ellis, K. Olive, Y. Santoso and V. Spanos, Phys. Lett. **B565** 176 (2003); U. Chattopadhyay, A. Corsetti and P. Nath, Phys. Rev. **D68** 035005 (2003).

[28] Talk by K. Woschnagg at the Neutrino 2004 Conference, Paris, June 14-19;
the AMANDA Collaboration: M. Ackermann, et al, astro–ph/0405218.

[29] I. Kravchenko, astro–ph/0306408.

[30] M. Birkel and S. Sarkar, Astropart. Phys. **9**, 297 (1998) [arXiv:hep-ph/9804285].

[31] C. L. Bennett *et al.*, Astrophys. J. Suppl. **148**, 1 (2003) [arXiv:astro-ph/0302207]; D. N. Spergel *et al.* [WMAP Collaboration], Astrophys. J. Suppl. **148**, 175 (2003) [arXiv:astro-ph/0302209]; H. V. Peiris *et al.*, Astrophys. J. Suppl. **148**, 213 (2003) [arXiv:astro-ph/0302225].

[32] K. A. Olive, arXiv:astro-ph/0503065.

[33] M. Battaglia, A. De Roeck, J. R. Ellis, F. Gianotti, K. A. Olive and L. Pape, Eur. Phys. J. C **33**, 273 (2004) [arXiv:hep-ph/0306219].

[34] A. Heister *et al.* [ALEPH Collaboration], Phys. Lett. B **583** (2004) 247; A. Heister *et al.* [ALEPH Collaboration], Phys. Lett. B **544** (2002) 73 [arXiv:hep-ex/0207056].

[35] G. Belanger, S. Kraml and A. Pukhov, arXiv:hep-ph/0502079; B. C. Allanach, S. Kraml and W. Porod, JHEP **0303**, 016 (2003) [arXiv:hep-ph/0302102]; see also the URL http://cern.ch/kraml/comparison/

[36] G. Belanger, F. Boudjema, A. Pukhov and A. Semenov, arXiv:hep-ph/0405253; G. Belanger, F. Boudjema, A. Pukhov and A. Semenov, Comput. Phys. Commun. **149**, 103 (2002) [arXiv:hep-ph/0112278].

[37] F. E. Paige, S. D. Protopescu, H. Baer and X. Tata, arXiv:hep-ph/0312045.

[38] H. Lai et al., Phys. Rev. **D55** 1280 (1997).

[39] J. Learned, S. Pakvasa, Astropart. Phys. **3** 267 (1995).

[40] For example, see P. Fouque, J. M. Solanes, T. Sanchis and C. Balkowski, "Structure, mass and distance of the Virgo cluster from a Tolman-Bondi model", arXiv:astro-ph/0106261.

[41] S. Hannestad, hep–ph/0409108.